Processing and Structural Properties of Waxy Maize Starch Nanocrystals Reinforced Natural Rubber

ARTICLE *in* MACROMOLECULES · MAY 2005

Impact Factor: 5.8 · DOI: 10.1021/ma050054z

4 AUTHORS, INCLUDING:

Hélène Angellier-Coussy
Université de Montpellier
40 PUBLICATIONS **1,123** CITATIONS
SEE PROFILE

Sonia Molina-Boisseau
French National Centre for Scientific Research
35 PUBLICATIONS **1,189** CITATIONS
SEE PROFILE

Alain Dufresne
Grenoble Institute of Technology
312 PUBLICATIONS **15,283** CITATIONS
SEE PROFILE

Processing and Structural Properties of Waxy Maize Starch Nanocrystals Reinforced Natural Rubber

Hélène Angellier,[†] Sonia Molina-Boisseau,[†] Laurent Lebrun,[‡] and Alain Dufresne*[,§]

Centre de Recherches sur les Macromolécules Végétales (CERMAV-CNRS), Université Joseph Fourier, BP 53, 38041 Grenoble Cedex 9, France; Polymères, Biopolymères, Membranes (PBM-CNRS), Université de Rouen, 76821 Mont-Saint-Aignan Cedex, France; and Ecole Française de Papeterie et des Industries Graphiques de Grenoble (EFPG-INPG), BP 65, 38402 St Martin d'Hères Cedex, France

Received January 11, 2005; Revised Manuscript Received February 9, 2005

ABSTRACT: Nanocomposite materials were obtained using a latex of natural rubber as the matrix and an aqueous suspension of waxy maize starch nanocrystals as the reinforcing phase. Starch nanocrystals were obtained after sulfuric acid hydrolysis of waxy maize starch granules. They consisted of crystalline platelets 6−8 nm thick, 40−60 nm long, and 15−30 nm wide. After mixing the latex and the starch nanocrystals, the resulting aqueous suspension was cast and evaporated. The solid nanocomposite films were characterized using scanning electron microscopy, water and toluene absorption experiments, differential scanning calorimetry, and wide-angle X-ray diffraction analysis. The barrier properties of the nanocomposites to water vapor and oxygen were also investigated, and the effect of surface chemical modification of starch nanocrystals was studied.

Introduction

There is currently a considerable interest in processing polymeric composite materials filled with rigid particles having at least one dimension in the nanometer range. This class of material attracting both scientist and industrial communities is called "nanocomposites." Because of the nanometric size effect, these composites display some unique outstanding properties with respect to their conventional microcomposite counterparts. Nowadays, the development of new nanocomposite materials are restricted by both the limited availability of nanoparticles and their strong tendency to aggregate, preventing their homogeneous dispersion within a continuous matrix, which is the key step required for high mechanical performances.

In the context of both biomass valorization and nanocomposite materials development, starch nanocrystals obtained by acid hydrolysis of potato and waxy maize starch granules have been used as a filler in a synthetic polymeric matrix and appeared to be an interesting reinforcing agent.[1−3] Several reasons led to a growing interest in the nonfood usage of starch-based products for applications in which synthetic polymers have traditionally been the materials of choice. Starch is a natural polymer, and it is available in large amounts from many renewable plant sources. It is the cheapest biopolymer produced beyond markets, and it is totally biodegradable. Furthermore, compared to rodlike nanocrystals extracted from cellulose or chitin, starch nanocrystals present the originality to have a platelet-like morphology. They consist of crystalline nanoplatelets about 6−8 nm thick with a length of 20−40 nm and a width of 15−30 nm.[4] The preparation of such nanocrystals was earlier reported by Batista.[5] However, the main drawbacks for the more extensive use of such nanoplatelets in nanocomposite applications were the duration (40 days of treatment) and the yield (0.5 wt %) of the HCl hydrolysis step. To lift the problem of availability, a previous work consisted in optimizing the preparation of nanocrystals from waxy maize granules in order to extend their use in nanocomposite applications.[6]

The focus of this work was to process nanocomposite materials consisting of natural rubber filled with waxy maize starch nanocrystals. Nowadays, carbon black (manufactured by burning oil or natural gas in controlled conditions) is the most important reinforcing agent used in the rubber industry. In the past decades, research was focused on the development of other reinforcing agents to replace carbon black in rubber compounds. In fact, because of its origin from petroleum, carbon black causes pollution and gives to the rubber a black color. Kaolin and silica were commonly used as reinforcing agents, but their reinforcing properties are lower than those obtained with carbon black. More recently, a variety of clays have been used to obtain unusual nanocomposites by exploiting the ability of the clay silicate layers to disperse into polymer matrices. The use of clay minerals such as montmorillonite[7] and organoclays[8−12] has been extended to natural rubber, and they seem to be a potential substitute to carbon black. Recently, Novamont (Novara, Italy), working in partnership with Goodyear Tire and Rubber, has developed tires using nanoparticles derived from corn starch, partially replacing the conventional carbon black and silica used in making tires.[13] This patented innovation, called Biotred, presents environmental advantages but also allows reducing the rolling resistance of tires. In this approach, waxy maize starch nanocrystals constitute another possible filler for natural rubber.

In the present work, these new nanocomposites, i.e., natural rubber filled with waxy maize starch nanocrystals, were characterized in terms of morphology, swelling behavior, barrier properties to water vapor and oxygen, thermal properties, and crystallinity. The effect of surface chemical modification of nanocrystals was also investigated.

[†] CERMAV-CNRS.
[‡] PBM-CNRS.
[§] EFPG-INPG.
* Corresponding author: e-mail Alain.Dufresne@efpg.inpg.fr.

10.1021/ma050054z CCC: $30.25
Published on Web 03/24/2005

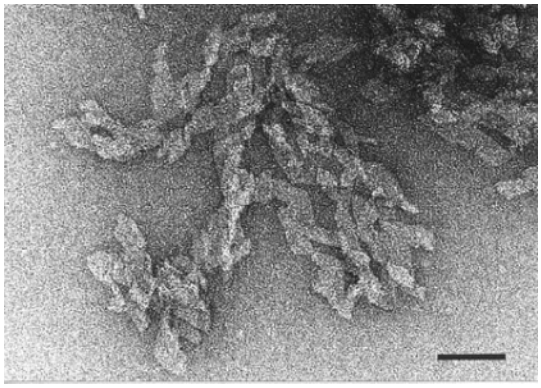

Figure 1. Transmission electron micrograph of negatively stained waxy maize starch nanocrystals. Scale bar: 50 nm.

Experimental Section

Waxy Maize Starch Nanocrystals. The preparation of waxy maize starch nanocrystals (labeled WN) by sulfuric acid (H_2SO_4) hydrolysis of native waxy maize starch granules (Waxylis, Roquette S.A., Lestrem, France) was optimized and described previously.[6] Briefly, 36.725 g of native waxy maize starch granules was mixed with 250 mL of 3.16 M H_2SO_4 for 5 days at 40 °C, with a stirring speed of 100 rpm. The suspension was washed by successive centrifugations with distilled water until neutrality. Resulting aqueous suspensions had a weight concentration of about 3.4 wt %. Waxy maize starch nanocrystals consist of platelet-like particles with a thickness of 6−8 nm, a length of 40−60 nm, a width of 15−30 nm, and a density, ρ_s, measured by BET (theory of Brunauer, Emmett, and Teller) of 1.55 g cm^{-3}, in agreement with the density reported in the literature for the crystalline part of starch.[14] Such nanocrystals are generally observed in the form of aggregates (Figure 1) having an average size around 4.4 μm, as measured by laser granulometry.[6] The specific surface measured by BET was found to be equal to 3.23 m^2 g^{-1}, proving that platelets are not individual (we should have a specific surface equal to 230 m^2 g^{-1} for perfectly individualized particle and assuming average dimensions) but also not compact spherical aggregates with a diameter of 4.4 μm (for which we should have a specific surface of 0.88 m^2 g^{-1}). However, it is worth noting that the experimental specific surface was determined by BET using a freeze-dried suspension of starch nanocrystals. The freeze-drying process most probably induced an aggregation phenomenon of the particles, leading to an underestimated value of the specific surface. Despite the micrometric scale of the starch nanoparticles, the term nanocomposite is suitable for starch nanocrystals/NR materials since the primary particles are nanometric, as for carbon black filled materials. In addition, we can suppose that at least one of the dimensions of the aggregates is at the nanometer scale.

The surface of freeze-dried starch nanocrystals was chemically modified as described in a previous paper.[15] The two grafting agents used were a commercial alkenyl succinic anhydride (ASA, Accosize 18 from American Cynamid) and phenyl isocyanate. The modified particles appeared as a powder after extraction.

Natural Rubber. Natural rubber (NR) was kindly supplied as NR latex by the Technical Center MAPA (Liancourt, France). It contained spherical particles with an average diameter around 1 μm, and its weight concentration was about 50 wt %. The density of dry NR, ρ_{NR}, was 1 g cm^{-3}, and it contained more than 98% of *cis*-1,4-polyisoprene.

Film Processing. *NR Latex/Starch Nanocrystals.* The aqueous suspension of starch nanocrystals and the latex were mixed in various proportions in order to obtain dry films between 200 μm and 1 mm thick depending on the test and with weight fractions of dry starch nanocrystals (w_s) within the NR matrix ranging from 0 to 50 wt %. After mixing, the mixtures were stored under vacuum and stirred on a rotavapor during about 10 min in order to degasse the mixture and thereby avoid the formation of irreversible bubbles during the water evaporation step. Then, the preparations were cast in Teflon molds and evaporated at 40 °C in a ventilated oven for 6−8 h (depending on the water content) and then heated at 60 °C under vacuum for 2 h. Resulting films were conditioned at room temperature in desiccators containing P_2O_5 salt until being tested.

Table 1. Codification of the Samples

sample	filler	medium	starch content (wt %)	starch content (vol %)[a]
L100		water	0	0
LT100		toluene	0	0
L98	unmodified	water	2	1.29
L95			5	3.28
L90			10	6.69
L85			15	10.2
L80			20	13.9
L75			25	17.7
L70			30	21.7
L60			40	30.1
L50			50	39.2
ASA5	ASA-modified	toluene	5	3.28
ASA10			10	6.69
ASA20			20	13.9
ASA30			30	21.7
PI5	PI-modified	toluene	5	3.28
PI10			10	6.69
PI20			20	13.9
PI30			30	21.7

[a] Assuming densities of starch nanocrystals and NR as 1.55 and 1 g cm^{-3}, respectively.

Solubilized NR/Modified Starch Nanocrystals. For the processing of composite materials filled with chemically modified starch nanocrystals, the latex of natural rubber was first dried in an oven and then solubilized in an excess of toluene. A strong mechanical dispersion treatment with Ultra-Turrax (IKA, Staufen, Germany) was necessary to completely solubilized natural rubber. The resulting solution had a weight concentration around 2.5 wt %. After being dispersed in toluene under magnetic stirring for 1 h, modified starch nanocrystals were mixed with the NR solution. Then, toluene was evaporated on a rotavapor until obtaining a thick slurry. The mixtures were cast in glass mold covered with aluminum foil laminated with Teflon FEP film (Bypac, Saint-Gobain) and evaporated at 40 °C in a ventilated oven for 6−8 h depending on the toluene content. Finally, the dry films were heated at 60 °C under vacuum for 2 h and stored at room temperature in desiccators containing P_2O_5 until being tested.

Samples codifications used in this study are listed in Table 1.

Scanning Electron Microscopy. Scanning electron microscopy (SEM) was performed with a JEOL JSM-6100 microscope (Tokyo, Japan). The samples were frozen under liquid nitrogen, then fractured, mounted, coated with gold/palladium on a JEOL JFC-1100E ion sputter coater, and observed. SEM micrographs were obtained using 8 kV secondary electrons.

Small-Angle Light Scattering. Small-angle light scattering was performed with a red laser ($\lambda = 630$ Å) and a precision cell having a light path of 1 mm. The scattered light intensity was picked up with a camera Micam VHR 1000, and images were recorded every 240 s.

Toluene and Water Uptake. The kinetics of toluene and water absorption was determined for all compositions. The specimens were squared films with dimensions around 10 × 10 × 0.2 mm^3. The films were thin enough so that the diffusion was supposed to be unidirectional. After being weighted using a four-digit balance, the samples were immersed in distilled water or toluene. The samples were removed at specific intervals and weighted. The water uptake (WU) as well as toluene uptake (TU) was calculated as follows:

$$\mathrm{WU}\ (\%) = \frac{m_t - m_0}{m_0} \times 100 \qquad (1)$$

where m_0 and m_t are the weights of the samples before and after a time t of immersion, respectively.

The mass of solvent absorbed at time t can be expressed as[16]

$$\frac{m_t - m_0}{m_\infty} = 1 - \sum_{\infty}^{n=0} \frac{8}{(2n+1)^2\pi^2} \exp\left[\frac{-D(2n+1)^2\pi^2 t}{4L^2}\right] \quad (2)$$

where m_∞ is the weight of the sample at the equilibrium, $2L$ the thickness of the film, and D the diffusion coefficient. At short times, this equation can be written as

$$\frac{m_t - m_0}{m_\infty} = \frac{2}{L}\left(\frac{D}{\pi}\right)^{1/2} t^{1/2} \quad (3)$$

For $(m_t - m_0)/m_\infty \leq 0.5$, the error in using eq 3 instead of eq 2 to determine the diffusion coefficient is about 0.1%.[17] The plots of $((m_t - m_0)/m_\infty)^2$ as a function of $(4t/(\pi L^2))$ were drawn for all compositions and $(m_t - m_0)/m_\infty \leq 0.5$. The diffusion coefficients were calculated from the slope of these plots.

The fraction of NR bonded to the filler and the fraction of NR dissolved in toluene were determined by the following procedure. Samples with dimensions around $10 \times 10 \times 1$ mm^3 were first weighed (M_0), then immersed in toluene for 48 h, dried overnight at 40 °C, and finally weighed again (M_0'). The relative weight loss (RWL = $(M_0 - M_0')/M_0$), the insoluble fraction of the composite material (IF = (1 − RWL)), the insoluble fraction of the NR matrix (IFM = $(1 - \mathrm{RWL}_0)(1 - w_s)$), where RWL_0 is the relative weight loss of the unfilled matrix and w_s is the weight fraction of starch), and the expected soluble part of the matrix (SFM = $\mathrm{RWL}_0(1 - w_s)$) were then determined. The starch nanocrystals loss, labeled SL, was finally calculated as the difference between the RWL and the expected soluble part of the matrix.

Barrier Properties. Barrier properties were tested for NR latex filled with unmodified waxy maize starch nanocrystals composite films only.

Permeability to Water Vapor. The water vapor transmission rate (g m^{-2} day^{-1}) was measured for circular films filled with 5, 10, and 20 wt % of starch, with a diameter of 9 cm. Each specimen was sealed on test cups containing a desiccant (anhydrous $CaCl_2$). The tests were performed in controlled temperature and humidity atmosphere (23 °C, 50% RH). The cups were weighed twice a day for 1 week. For each set of samples, a reference was used to determine the quantity of water vapor retained by the film itself. It consisted of a film sealed on a salt-free cup.

Permeability to Oxygen. The permeability of the films to oxygen was determined using the permeation apparatus previously described.[18] Before any measurement, the permeation cell was completely evacuated by applying vacuum on both sides of the film overnight. Then, the upstream side was provided with the gas under test at pressure, $p_1 = 3$ bar. The increase of pressure, p_2, in the calibrated downstream volume was measured using a sensitive pressure gauge (0−10 mbar, Effa AW-10-T4) linked to a data acquisition system. The permeability coefficient ($P = J_{st}L/p_1$) was calculated using the variable pressure method[19] assuming $p_1 \gg p_2$, where L is the sample thickness and J_{st} the steady-state gas flux obtained from the slope of the steady-state part of the curve p_2 vs time. A time lag diffusion coefficient ($D = L^2/6t_L$) was calculated from the time lag, t_L, given by the intercept of the steady-state asymptote on the time axis. The solubility coefficient, S, was given by the ratio of the permeability to diffusion coefficients. For each film, the permeation experiments were duplicated. Therefore, the permeation parameters (P, D, S) were obtained with an accuracy ranging from 5% to 10% and averaged.

Differential Scanning Calorimetry (DSC). Differential scanning calorimetry measurements were done with a TA Instruments (New Castle, DE) calorimeter (DSC 2920 modulated DSC), fitted with a cooler system using liquid nitrogen. Each sample was heated from −110 to 0 °C with a heating rate of 10 °C min^{-1}. The glass−rubber transition was characterized by three different temperatures in the DSC traces (Figure 2), i.e., (i) T_{g1}, corresponding to the onset of the specific heat increment ascribed to T_g, in others words, the temperature at which some polymer chains start to undergo the transition; (ii) T_{g2}, which is associated with the temperature at which the differential heat flow is maximum; and (iii) T_{g3}, corresponding to the offset of the glass−rubber transition, i.e., the temperature at which the DSC curves join again the baseline.[20]

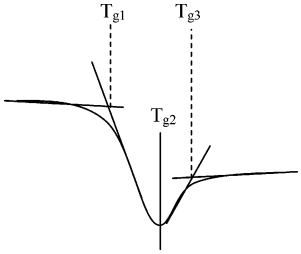

Figure 2. Manifestation of the glass−rubber transition of an amorphous polymer in DSC experiments and position of the characteristics temperatures.

X-ray Diffraction. Films were X-rayed for 2 h at room temperature and humidity (about 56% RH) using a Philips PW3830 generator operating at the Ni-filtered Cu Kα radiation wavelength ($\lambda = 1.542$ Å). Diffraction patterns were recorded on Fuji imaging plates read by a Fuji BAS 1800 II phosphoimager. The profiles of the diffraction patterns were obtained using the Scion Image software.

Results and Discussion

Morphology of Nanocomposite Films. The morphology of NR/starch nanocrystals materials and the distribution level of the filler within the matrix were evaluated by observing the surface of fractured films using SEM. Figure 3 shows the surface of unfilled NR (Figure 3a) and films filled with 5 wt % (Figure 3b) and 30 wt % (Figure 3c,d) of nanocrystals. The freshly fractured surface of the unfilled NR film (Figure 3a) is smooth and uniform. By comparing with the micrographs showing the surface of fracture of composites, it is easy to identify the filler. Starch nanocrystals appear like white dots, whose concentration is a direct function of the starch content in the composite. We can observe that the distribution of the filler among the matrix is homogeneous for both compositions. It is a key property for expecting good mechanical properties. Furthermore, no particular sedimentation phenomenon of starch nanocrystals within the thickness of the films was observed.

Small-angle light scattering experiments were performed on starch nanocrystals aqueous suspensions in order to evaluate the kinetic of sedimentation of the nanoparticles. Indeed, it was important to check whether they were able to sediment during the water evaporation step. Suspensions with starch content of 3.4 wt %, which was close to the concentration of aqueous starch nanoparticles suspensions used for the processing of nanocomposite films, were tested. It was shown that for any wave vector, i.e., any angle of diffusion, the intensity of scattered light did not decrease for a period of at least 12 h (Figure 4), revealing that there was no sedimentation of the nanocrystals during the evaporation step, which takes 6−8 h depending on the composition. In addition, this stability should be higher during the processing of nanocomposites because of the presence of the NR particles which should increase the viscosity of the mixture. In fact, the intensity of scattered light slightly increases, revealing that starch nanocrystals

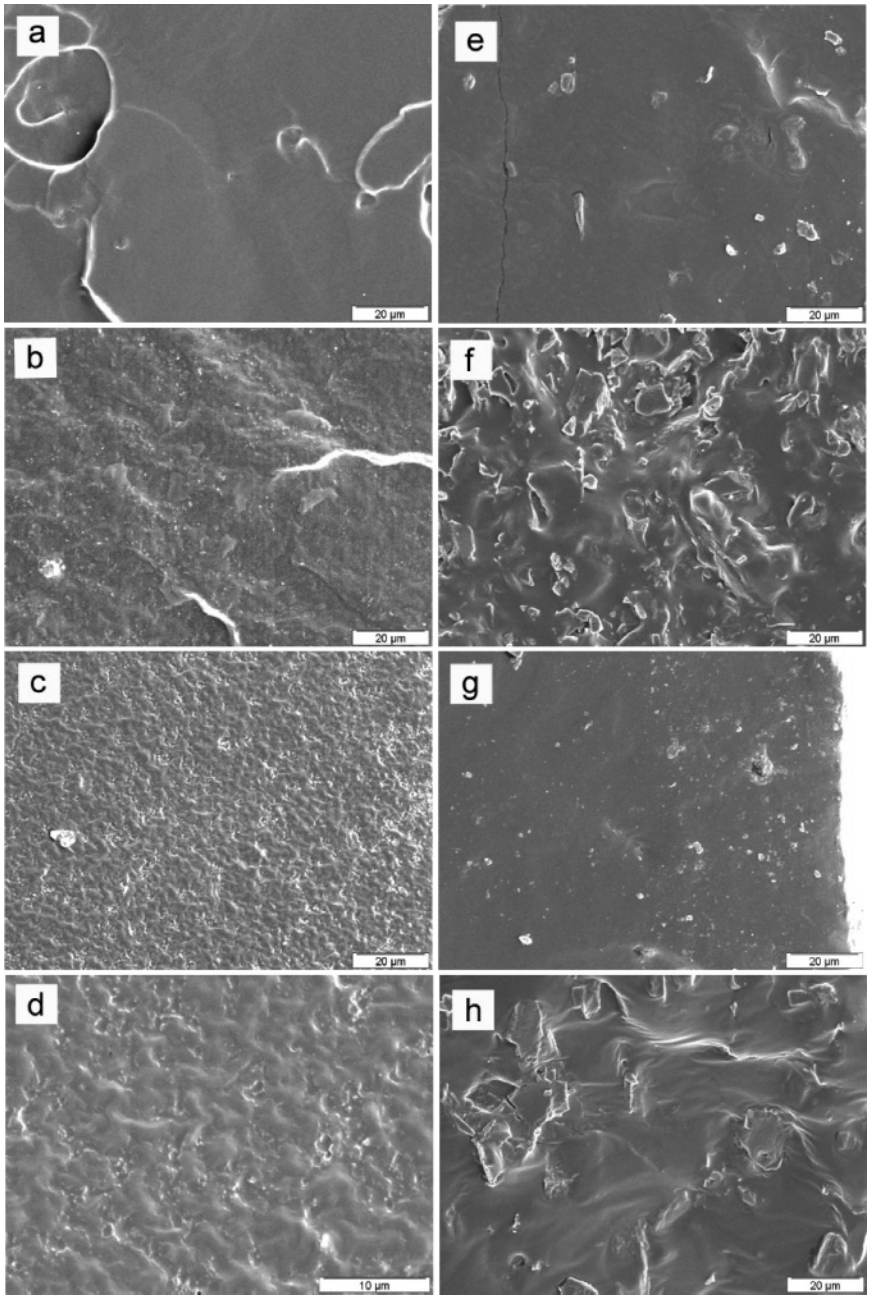

Figure 3. Scanning electron micrographs of the fractured surfaces of (a) unfilled NR, NR filled with (b) 5 and (c, d) 30 wt % of starch nanocrystals, NR filled with (e) 5 and (f) 30 wt % of ASA-modified particles, and NR filled with (g) 5 and (h) 30 wt % of PI-modified particles.

tend to aggregate in aqueous medium but not sufficiently to induce a sedimentation phenomenon.

The effect of the surface chemical modification on the dispersion level of the filler among the matrix is shown in Figure 3e−h. The dispersion of modified particles is clearly nonuniform. Aggregates of several microns and large smooth unfilled domains can be observed. The formation of these aggregates should be due to the extraction step of modified nanocrystals,[15] after which a compact powder was obtained.

Swelling Behavior. *Toluene Swelling Behavior.* In absorption kinetics experiments, the mass of sorbed solvent is measured as a function of time. Figure 5a displays the evolution of the toluene uptake (TU) vs time for different starch contents. All the compositions absorbed toluene during the experiment. Two zones can be distinguished. The first zone, corresponding to $t <$ 10 h, is characterized by fast absorption kinetics. A clear trend is observed with respect to the starch content: the higher the starch content is, the lower the absorption rate is. In the second zone, associated with long times of experiments, the toluene uptake increases more slightly until reaching a plateau corresponding to the toluene uptake at equilibrium. For low starch contents (0 and 2 wt %), the second zone is not observed. A disruption of part of the films due to their repetitive manipulations rapidly occurred, preventing their weighing after several hours of immersion. Thereby, the TU at equilibrium for L100 and L98 films was considered to be infinite. It is worth noting that only 5 wt % of starchy filler allows preventing the disruption of the matrix. The toluene uptake values at equilibrium were measured after 7 days of immersion (170 h) and are given in Table 2. We can notice that TU values at

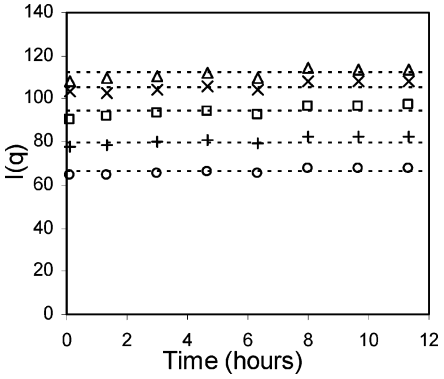

Figure 4. Evolution of the scattered light intensity vs time for different wave vectors (nm^{-1}), i.e., $q = 8.54 \times 10^{-4}$ (△), $q = 16.94 \times 10^{-4}$ (×), $q = 25.07 \times 10^{-4}$ (□), $q = 32.83 \times 10^{-4}$ (+), $q = 40.14 \times 10^{-4}$ (○), for a 3.4 wt % waxy maize starch nanocrystal aqueous suspension.

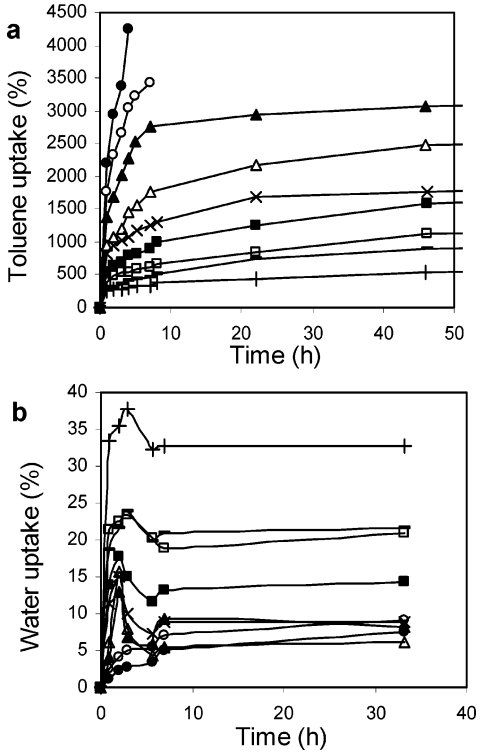

Figure 5. Evolution of (a) toluene uptake and (b) water uptake as a function of time at room temperature for L100 (●), L98 (○), L95 (▲), L90 (△), L85 (×), L80 (■), L70 (□), L60 (−), and L50 (+). Solid lines serve to guide the eyes.

equilibrium decrease continuously when increasing the starch content (Figure 6a).

The toluene diffusivities or diffusion coefficients of toluene, noted $D_{toluene}$, were estimated for all compositions. These values are collected in Table 2. The unfilled NR matrix displayed the highest toluene diffusion coefficient. Adding starch nanocrystals to the NR matrix first resulted in a dramatic decrease of the toluene diffusivity, followed by a more progressive linear decrease from 10 wt % of filler (Figure 6b).

All these results seem to show that starch nanocrystals may form a three-dimensional network, in agreement with TEM observations (Figure 1), that allows reducing the swelling capability of the matrix. The formation of this kind of network was already reported for rodlike polysaccharide fillers.[21,22] It was assumed to result from the establishment of strong hydrogen bonds between particles that can form during the evaporation process. The structure of starch nanocrystals is completely different, but one can assume that above a given volume fraction starch nanoparticle clusters can connect to form a continuous infinite and open network. This assumption is also supported by SEM observations (Figure 3a−d). The reduction of swelling upon starch nanocrystals addition could also be due to possible interactions between starch and natural rubber, thereby preventing the swelling of the polymeric chains located in the interfacial zone.

Table 2. Toluene Uptake (TU) at Equilibrium, Diffusion Coefficient of Toluene ($D_{toluene}$), Water Uptake (WU) at Equilibrium, and Diffusion Coefficient of Water (D_{water}) in Starch Nanocrystal/NR Nanocomposite Films Immersed in Toluene or Water

sample	TU at equilib (%)	$D_{toluene}$ ($cm^2\ s^{-1} \times 10^8$)	WU at equilib (%)	D_{water} ($cm^2\ s^{-1} \times 10^{10}$)
L100	∝	40	7	0.04
L98	∝	38	9	0.17
L95	3290	20.8	8	0.29
L90	2660	7.9	6	0.71
L85	2210	5.4	9	3.48
L80	2020	5.1	14	4.19
L70	1320	3.4	22	5.61
L60	1110	3.8	26	4.36
L50	750	1.6	33	13.7

The nanocomposite materials about 1 mm thick were immersed in toluene for 48 h, dried overnight at 40 °C, and weighed as described in the Experimental Section. The relative weight loss values, RWL, are given in Table 3. Data show that about 15 wt % of the unfilled matrix was dissolved in toluene after 48 h immersion. The dissolution of a limited amount of NR can be ascribed to the fact that the experiment was performed at room temperature without any stirring or repetitive manipulations. Furthermore, it is worth noting that the thick-

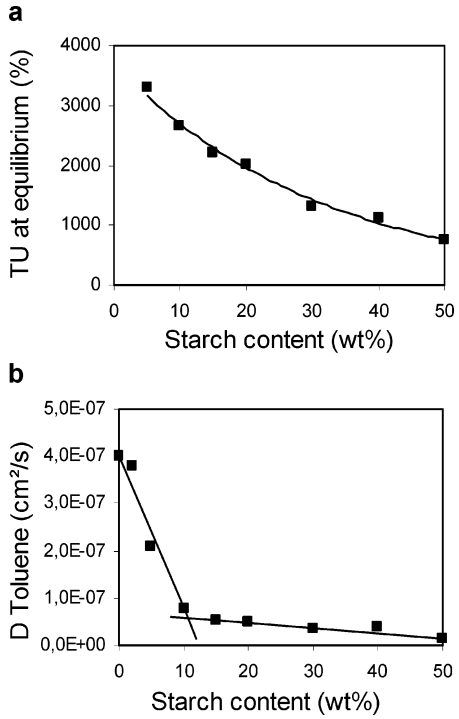

Figure 6. Evolution of (a) toluene uptake at equilibrium and (b) diffusion coefficient of toluene for starch nanocrystals/NR nanocomposite films as a function of starch content. The solid line serves to guide the eyes.

Table 3. Relative Weight Loss (RWL), Insoluble Fraction of the Composite (IF), Insoluble Fraction of the NR Matrix (IFM), Expected Soluble Fraction of the Matrix (SFM), and Starch Nanocrystals Loss (SL) of Starch Nanocrystal/NR Nanocomposite Films Immersed for 48 h in Toluene or in Water and Dried Overnight at 40 °C (Values Are Given in %)

medium	toluene					water	
sample	RWL[a]	IF[b]	IFM[c]	SFM[d]	SL[e]	RWL[a]	SL[e]
L100	14.6	85.4	85.4	14.6	0	3.1	0
L95	14	86.0	81.1	13.9	0	3.7	0.7
L90	22.6	77.4	76.8	13.2	9.4	4.8	2.0
L80	22.9	77.1	68.3	11.7	11.2	9.8	7.3
L70	26.3	73.7	59.8	10.3	16	10.2	8
L60	27.2	76.8	51.2	8.8	18.4	14.1	12.2
L50						15.8	14.3

[a] RWL = $(M_0 - M_0')/M_0 \times 100$, where M_0 and M_0' are the initial and final weights of the sample. [b] IF = 100 − RWL. [c] IFM = $(100 - \mathrm{RWL}_0)(1 - w)$, where RWL_0 is the RWL value of the unfilled NR matrix and w_s is the starch nanocrystals content (wt %). [d] SFM = $\mathrm{RWL}_0(1 - w_s)$. [e] SL = RWL − SFM.

ness of the films (around 1 mm) was in this case higher than those of the films used for diffusivity measurements (around 0.2 mm). It is observed that RWL increases for starch contents higher than 5 wt %. This result reveals that, contrary to what was observed for chitin whiskers filled NR,[21] the addition of starch nanocrystals does not prevent the dissolution of the matrix in toluene. RWL is systematically higher than the soluble fraction of the matrix, SFM. Thereby, assuming that the addition of filler cannot favor the dissolution of the matrix, it means that the loss in weight should be due to a loss of natural rubber but also of starch nanocrystals. Indeed, we have seen that during toluene immersion natural rubber swelled. Fillers are then surrounded by a soft matrix and are able to leave the specimen. In addition, this phenomenon should be aggravated for highly filled composites since the probability of appearance of starch nanocrystals on the surface of the film is more significant as the starch content is higher.[2] Observations of the samples clearly prove the migration of starch nanocrystals toward the surface: after extended immersion and drying, the surface is covered by a thin white layer. The values of the starch nanocrystals loss, SL, are given in Table 3. We can note that this loss of starch nanocrystals should be gradual during the swelling experiment because no particular break of slope is observed in the evolution of the toluene uptake. This is an indication that although the starch nanocrystal clusters seem to be involved in the formation of a continuous and open network, the interactions between these clusters should be weak and easily broken under NR matrix swelling.

Water Swelling Behavior. In a similar way as for toluene uptake experiments, the water uptake of soaked samples after immersion in distilled water at room temperature was plotted as a function of time (Figure 5b). Similarly to toluene experiments, we noted that all the compositions absorbed water during immersion, even the unfilled matrix. For low starch contents (0 and 2 wt %), the water uptake increased slightly during all the duration of the experiment. For starch contents higher than 2 wt %, the water uptake increased rapidly during the early stage of immersion, i.e., during the two or three first hours, and then decreased until reaching a plateau after 7 h of immersion. The diminution in the water uptake may be due to the partial release, or leaching, of starch nanoparticles in water, even though

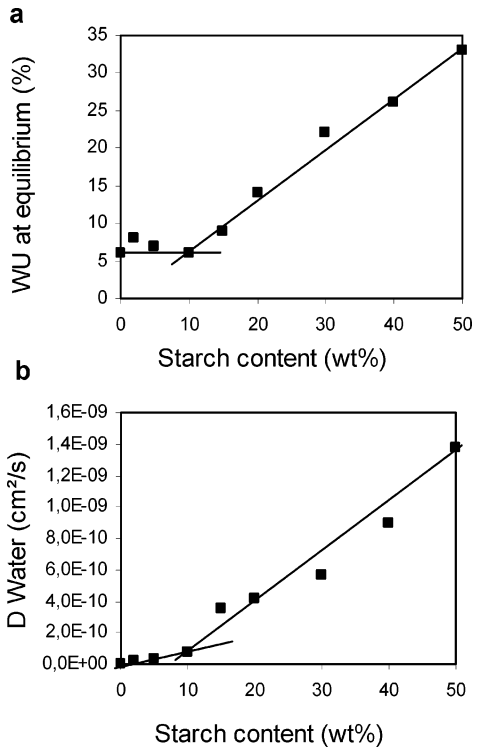

Figure 7. Evolution of (a) the water uptake at equilibrium and (b) the diffusion coefficient of water for starch nanocrystals/NR nanocomposite films as a function of starch content.

starch is insoluble in water. This phenomenon was already reported for polystyrene-*co*-butyl acrylate filled with potato starch microcrystals.[2]

To verify this assumption, samples (1 mm thick) were first weighed, then immersed in distilled water for 2 days, removed from water, dried at 40 °C overnight, and weighed again. The relative weight loss, RWL, was calculated for each sample, and results are given in Table 3. The RWL for L100 equals 3.1% most probably due to the release of low molecular mass NR chains. It was found to increase by adding starch nanoparticles, revealing that some starch nanocrystals have previously migrated toward the aqueous phase during soaking, as shown by SL values. The increase in RWL values became more significant above 10 wt % of filler. Indeed, we have seen that during exposure to water starch domains swelled, and the interface between filler and NR matrix weakens. Fillers should be then surrounded by a soft interface and can be able to leave the specimen. Furthermore, like for immersion in toluene, this phenomenon should be magnified for highly filled materials due to the increasing probability of appearance of starch nanocrystals on the surface of the film in direct contact with the liquid medium. Data show that the loss of starch nanocrystals is higher after immersion in toluene than in water. This is attributed to a more extended swelling of the matrix in toluene, favoring the migration of the filler toward the surface and then the liquid phase.

The water uptake values at equilibrium are collected in Table 2, and their evolution as a function of starch content is displayed in Figure 7a. Up to a starch content of 10 wt %, WU at equilibrium remained roughly constant. Then, it increased more or less linearly from 6% for the 10 wt % filled material (L90) up to 33% for the 50 wt % filled film (L50). For highly filled materials

it seems that the loss of unbonded starch nanoparticles was compensated by the swelling of the in bulk starch nanocrystals still bonded to the matrix.

The water diffusion coefficient values, noted D_{water}, are given in Table 2, and their evolution vs starch content is displayed in Figure 7b. The unfilled NR matrix displays the lowest value, and the addition of starch nanocrystals induces an increase in water diffusivity. Up to a starch content of 10 wt %, D_{water} increases slightly and then increases more rapidly and roughly linearly. Contrary to toluene swelling experiments and as expected, the formation of a continuous polar network of starch nanocrystals within the NR matrix seems to favor the swelling of the films by water.

A filler content of 10 wt % seems to be a critical value in the swelling behavior. By analogy with materials reinforced with cellulose whiskers, it was assumed that the formation of a rigid network of starch nanocrystals was governed by a percolation mechanism. The critical volume fraction of starch nanocrystals at the percolation is difficult to determine due to the ill-defined geometry of the percolating species but should be around 6.7 vol % (i.e., 10 wt %). This value is smaller than the value reported for polystyrene-*co*-butyl acrylate filled with potato starch microcrystals (around 20 vol %).[2] This difference may be due to a higher surface area of waxy maize starch nanocrystals and to the particular morphology of starch nanocrystals that aggregate by forming a "lace net". This value is of the same order of magnitude (4.4 vol %) than the one observed for NR reinforced with chitin whiskers obtained from crab shell presenting a high specific surface around 180 $m^2\ g^{-1}$ and an aspect ratio close to 16.[22]

Influence of the Chemical Modification on Swelling Behavior. Water and toluene absorption experiments were carried out for unfilled NR (LT100) and relative composites filled with 10 and 30 wt % of ASA or PI-modified starch nanocrystals (ASA10, ASA30, PI10, and PI30) in order to study the effect of the surface chemical modification on swelling properties.

The problem we were faced to was the disruption of films filled with modified starch nanoparticles during the early stage of the swelling experiment after only 1 or 2 h of immersion in toluene depending on the filler content. This could be attributed to the film processing mode. Indeed, the solubilization step in toluene involved a mechanical stirring, which could result in a decrease of the molecular weight of the sample. For this reason, experiments were carried out by weighing swelled films every 15 min for 1 h. The values of TU obtained by weighing the sample after 1 h of immersion and those obtained after four weighing steps every 15 min cannot be compared (samples were removed from the liquid phase for 2 min during each weighing step).

The evolution of toluene uptake vs time at room temperature for these materials is displayed in Figure 8a. The data corresponding to the unfilled matrix obtained from the latex of NR (L100) and to NR film filled with 10 and 30 wt % of unmodified filler (L90 and L70) are added for comparison. It is clear that, whatever the composition, the swelling rate is systematically higher for NR/modified starch than for NR/unmodified nanocrystals. As discussed above, the addition of unmodified filler resulted in a diminution of the nanocomposites swelling. It was assumed that this phenomenon was due to the formation of a continuous network

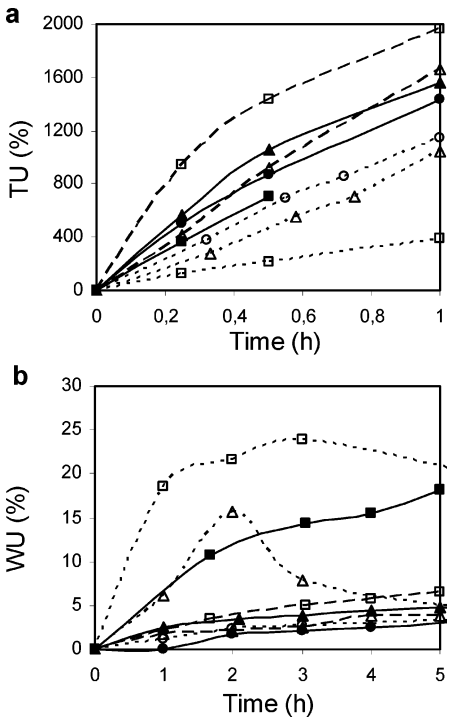

Figure 8. Evolution of (a) toluene uptake and (b) water uptake vs time at room temperature for LT100 (●), ASA10 (▲), ASA30 (■), PI10 (△), PI30 (□), L100 (−○−), L90 (−△−), and L70 (−□−). Lines serve to guide the eyes.

of starch nanoparticles supposed to be held through hydrogen-bonding forces between starch nanocrystals. In the case of the addition of modified filler, the swelling rate of the composite films is barely higher than for the unfilled NR matrix. This could be due to lower interactions between modified nanocrystals, to higher interactions between the filler and the matrix, or to a higher affinity between the modified filler and toluene. The TU is higher for materials filled with nanocrystals modified by PI than by ASA, revealing either a higher affinity of PI with toluene or lower interactions between modified nanoparticles.

The evolution of the water uptake for the same materials is displayed in Figure 8b. As expected, the water uptake is much lower for modified filler-based composites compared with its unmodified counterparts and is also lower for particles modified with PI than with ASA. Indeed, it was shown in a previous paper[15] that the polar component of surface energy was lower for modified particles and also much lower for particles modified with PI than with ASA.

Barrier Properties. *Permeability to Water Vapor.* According to the results of water uptake, we could have thought that the permeability to water vapor would also increase by adding starch nanocrystals due to their interconnection and thereby the most likely formation of a continuous starch pathway. However, we note that the water vapor transmission rate (WVTR) decreases continuously upon starch nanocrystals addition (Table 4). The hydrophilic nature of starch nanocrystals does not affect the permeability of natural rubber to water vapor. The morphological nature and platelet-like structure of starch particles have most probably an incidence on this result.

Permeability to Oxygen. Starch nanocrystals also reduced the oxygen diffusion through the nanocomposite films as shown from the decrease of D values upon filler

Table 4. Water Vapor Transmission Rate (WVTR), Diffusion Coefficient (*D*), Permeability Coefficient (*P*), and Solubility (*S*) of Oxygen for Starch Nanocrystal/NR Nanocomposite Films

sample	WVTR (g m^{-2} day^{-1})	D (cm^2 s^{-1} × 10^7)	P (barrer)[a]	S (cm^3 STP cm^{-1} Hg cm^{-3} × 10^3)
L100	0.078	16.3	25.7	1.58
L95	0.055			
L90	0.054	15.2	21.1	1.39
L80	0.043	10.2	16.8	1.65
L70		7.2	8.9	1.23

[a] 1 barrer = 10^{-10} cm^3 STP cm s^{-1} cm^{-2} cmHg^{-1}.

content increase in Table 4. It is believed that the platelet-like low permeable structures of the starch stand in the way of the oxygen molecules (O_2 diameter = 3.47 Å), increasing the tortuosity of the diffusion path. This effect was more marked for nanocrystals content up to 10 wt %. The unfilled NR film (L100) displays the highest P (P_{NR}) value, in agreement with the literature data for *cis*-1,4-polyisoprene (P = 37.5 barrer[23]). The addition of starch nanocrystals also reduces the oxygen permeability (Table 4). The relative permeabilities P_C/P_{NR} where P_C is the composite permeability are respectively 0.82, 0.65, and 0.34 for L90, L80, and L70 samples. The higher the starch content is, the higher the decrease of oxygen permeability is: 17.9% for 10 wt % starch nanoparticles filled NR (L90), 20.3% with 10 wt % more (L80), and 47% with 10 wt % more (L70). The decrease in P values could be related to the decrease in the diffusion coefficient D due to the structural modification of the film matrix and also to the decrease of the solubility. According to our results, the solubility values remain constant (if experimental errors are taken into account) except for L70. D values decrease more rapidly than S values as the starch content increases. Thus, the decrease in P is mainly due to the barrier effect of the starch (P = 3.2 barrer[24]). The high decrease of permeability of natural rubber filled with 30 wt % of starch nanocrystals is due to a large decrease of S that adds to the barrier effect.

Thermal Analysis. Differential scanning calorimetry (DSC) measurements were performed for all the NR/unmodified starch nanocrystals compositions. For all the samples, two successive temperature scans were recorded, and they were perfectly superimposed and reproducible. The DSC traces corresponding to the first temperature scan are shown in Figure 9.

The glass−rubber transition of unfilled NR occurred at an onset temperature T_{g1} of −66.6 °C and was followed by an endothermal peak. By adding starch nanocrystals, the magnitude of the specific heat increment at T_g obviously decreased as well as the endothermal peak (Figure 9). It is simply ascribed to the decreasing amount of NR matrix.

The evolution of the different characteristic temperatures as referred in the Experimental Section, viz. T_{g1}, T_{g2}, and T_{g3}, as a function of the starch content is displayed in Figure 10. The onset glass transition temperature T_{g1} decreased steadily when increasing the starch content while T_{g3} remained constant for all compositions. It means that the glass−rubber transition occurred on a broader temperature range for composites. In a first approach, we would have thought that the network formed by hydrogen bonding between nanocrystals and/or the interactions between the filler and the matrix would have hindered the motion of the polymeric chains and thereby delayed the onset temperature of the glass transition. The temperature associated with the maximum differential heat flow, T_{g2}, remained first constant around −62 °C for composite materials filled up to 25 wt % starch nanocrystals and then decreased down to −64.6 °C for the 50 wt % filled material.

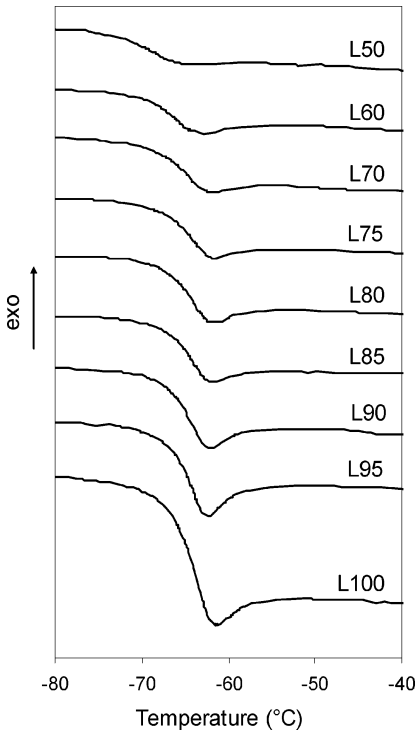

Figure 9. DSC thermograms of starch nanocrystals/NR nanocomposite films.

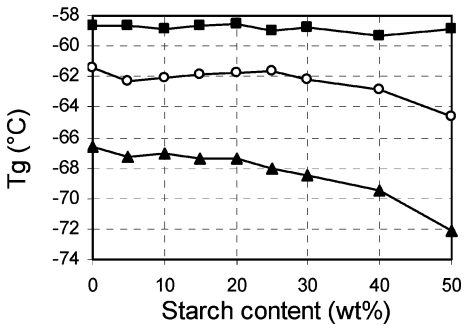

Figure 10. Evolution of T_{g3} (■), T_{g2} (○), and T_{g1}(▲) as a function of starch content. Lines serve to guide the eyes.

T_g values were similar for L100 and LT100 and were not affected upon addition of 20 or 30 wt % of ASA or PI-modified starch nanoparticles. Therefore, chemically modified particles did not affect the long-range cooperative motions of the polymeric chains. This means that among the two explanations retained to explain the peculiar swelling behavior of modified starch nanocrystal-based composites compared to unmodified ones, viz., lower interparticle interactions and higher NR−starch interactions, the former seems to be predominant (because if there were some interactions between NR and starch, this would have probably hindered the motion of the NR chains).

Structural Analysis. *Influence of Starch Content.* The nanocomposite films NR/starch nanocrystals were characterized by X-ray diffraction. X-ray patterns were collected for different compositions and are displayed in Figure 11. The diffractograms of unfilled natural

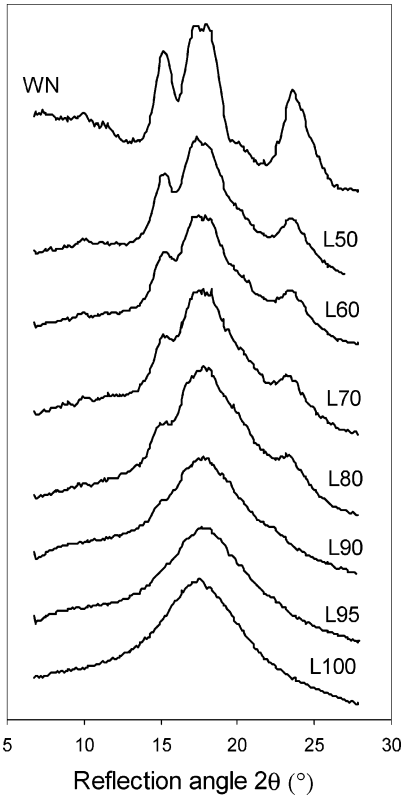

Figure 11. X-ray diffraction patterns of starch nanocrystals/NR nanocomposite films.

rubber and pure waxy maize starch nanocrystal films were added as references. The diffraction pattern recorded for a film of pure waxy maize starch nanocrystals obtained by pressing freeze-dried nanocrystals displays typical peaks of A-type amylose allomorph.[25] It is characterized by two weak peaks at $2\theta = 10.1°$ and 11.5°, a strong peak at 15.3°, a double strong peak at 17.1° and 18.2°, and a strong peak at 23.5°.

The natural rubber film (L100) displays a typical behavior of a fully amorphous polymer. It is characterized by a broad hump located around $2\theta = 18°$.

By adding starch nanocrystals, the peaks corresponding to A-type amylose allomorph become stronger and stronger, as expected. This shows that an increase of the starch content results in an increase of the global crystallinity of the composite material. The diffraction patterns of the various NR/starch nanocrystals do not exactly correspond to a simple mixing rule of the diffractograms of the two pure parent components, i.e., $I = w_s I_{WN} + (1 - w_s) I_{L100}$ where I is the diffracted intensity at each angle for a given composite film. Indeed, the experimental double central peak is stronger than the predicted one (not shown in this paper). This probably results from the different orientation of starch nanocrystals within the film obtained from only starch and from the composite. The nanocrystals distribution is most likely random in the composite contrarily to the reference starch nanoparticles films, which is composed of in-plane oriented filler.

Furthermore, X-ray analysis confirmed that the processing by casting and evaporation at 40 °C did not affect the crystallinity of the starch nanocrystals.

Influence of Humidity. Films with different starch contents were stored in a 98% RH (relative humidity) atmosphere for 2 weeks in order to evaluate the influence of the water content on the crystallinity of the studied composite materials. The peaks of diffraction for WN are stronger and more accurately defined in highly moist atmosphere (Figure 12), what is already well-known.[26] The effect of humidity is less and less marked with decreasing starch content. Indeed, we have seen that natural rubber is not permeable to water, preventing the migration of water toward the crystalline starchy zones of the composites.

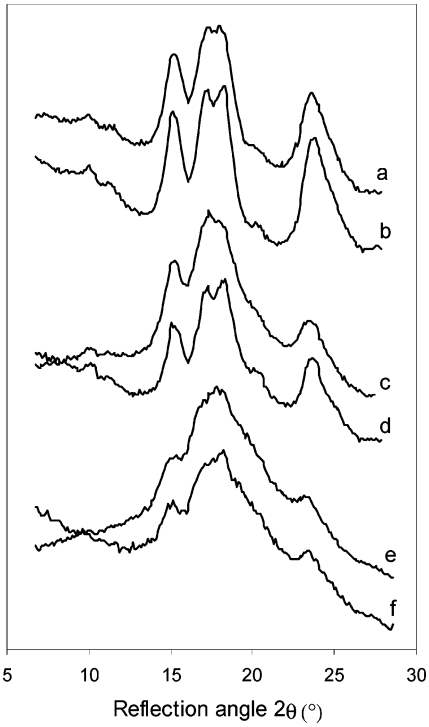

Figure 12. X-ray patterns of WN (a, b), L50 (c, d), and L80 (e, f) stored at 56% RH (a, c, e) and 98% RH (b, d, f).

Conclusion

Nanocomposite materials were obtained by casting and evaporating a mixture of NR latex (matrix) and aqueous suspension of waxy maize starch nanocrystals (filler). SEM observations confirmed that the filler was evenly distributed within the NR matrix, what is a key property for expecting good mechanical properties. Wide-angle X-ray diffraction analysis showed that the processing did not affect the crystallinity of the starch nanocrystals. By adding starch nanocrystals in NR, the swelling by toluene decreases and the swelling by water increases. It was assumed that these phenomena were due to the formation of a starch nanocrystals network through hydrogen linkages between starch nanoparticles clusters and also to favorable interactions between the matrix and the filler. It seems that the formation of the network of starch nanocrystals is governed by a percolation mechanism. Although not easily determinable due to the ill-defined geometry of the percolating species, the critical volume fraction of starch nanocrystals at the percolation should be around 6.7 vol % (i.e., 10 wt %). The platelet-like morphology of starch nanocrystals seems to be responsible for the decrease of both the permeability to water vapor and oxygen of natural rubber filled films. The surface chemical modification of starch nanocrystals results in a favored swelling behavior with toluene and a diminution of the water uptake. The mechanical properties of these nanocomposite materials will be discussed in the second part of this paper.

Acknowledgment. The authors are grateful to the Technical Centre, MAPA Co. (Liancourt, France) for the supply of NR latex and Roquette Frères (Lestrem, France) for the gift of native waxy maize starch granules. We thank Mrs. D. Dupeyre (CERMAV, France) for her help in SEM study and Dr. Cyrille Rochas (CERMO, Grenoble, France) for his support in small-angle light scattering measurements. Finally, we gratefully acknowledge Technical Paper Center (CTP, Grenoble) for water vapor permeability analysis.

Note Added after ASAP Publication. This article was released ASAP on March 24, 2005. Figures 9 and 12 have been revised. Sentence 8 in the first paragraph of the Experimental Section has been revised and the last sentence in paragraph 12 of the Results and Discussion has been revised. The revised version was posted on March 31, 2005.

References and Notes

(1) Dufresne, A.; Cavaillé, J. Y.; Helbert, W. *Macromolecules* **1996**, *29*, 7624−7626.
(2) Dufresne, A.; Cavaillé, J. Y. *J. Polym. Sci., Part B: Polym. Phys.* **1998**, *36*, 2211−2224.
(3) Angellier, H.; Molina-Boisseau, S.; Putaux, J. L.; Dupeyre, D.; Dufresne, A. *Macromol. Symp.* **2005**, *221*, 95−104.
(4) Putaux, J. L.; Molina-Boisseau, S.; Momaur, T.; Dufresne, A. *Biomacromolecules* **2003**, *4*, 1198−1202.
(5) Battista, O. A. In *Microcrystal Polymer Science*; McGraw-Hill Book Co.: New York, 1975; p 138.
(6) Angellier, H.; Choisnard, L.; Molina-Boisseau, S.; Ozil, P.; Dufresne, A. *Biomacromolecules* **2004**, *5*, 1545−1551.
(7) Vu, Y. T.; Mark, J. E.; Pham, L. H.; Engelhardt, M. *J. Appl. Polym. Sci.* **2001**, *82*, 1391−1403.
(8) Okada, A.; Usuki, A.; Kurauchi, T.; Kamigaito, O. In *Hybrid Organic−Inorganic Composites*; Mark, J., Lee, C., Bianconi, P., Eds.; *ACS Symp. Ser.* **1995**, 55−65.
(9) Arroyo, M.; Lopez-Manchado, M. A.; Herrero, B. *Polymer* **2003**, *44*, 2447−2453.
(10) Joly, S.; Garnaud, G.; Ollitrault, R.; Bokobza, L. *Chem. Mater.* **2002**, *14*, 4202−4208.
(11) Kim, J. T.; Oh, T. S.; Lee, D. H. *Polym. Int.* **2004**, *53*, 406−411.
(12) Bala, P.; Samantaray, B. K.; Srivastava, S. K.; Nando, G. B. *J. Appl. Polym. Sci.* **2004**, *92*, 3583−3592.
(13) Materne, T.; Corvasce, F.; Leitz, P. EP995775A1, European patent, 2000.
(14) Donovan, J. W. *Biopolymers* **1979**, *18*, 263−275.
(15) Angellier, H.; Molina-Boisseau, S.; Belgacem, M. N.; Dufresne, A. *Langmuir* **2005**, *21*, 2425−2433.
(16) Comyn, J. In *Polymer Permeability*; Comyn, J. E., Ed.; Elsevier Applied Science: New York, 1985.
(17) Vergnaud, J. M. In *Liquid Transport Process in Polymeric Materials: Modeling and Industrial Applications*; Prentice-Hall: Englewood Cliffs, NJ, 1991.
(18) Joly, C.; Le Cerf, D.; Chappey, C.; Langevin, D.; Muller, G. *Sep. Pur. Technol.* **1999**, *16*, 47−54.
(19) Glatz, F. P.; Mulhaupt, R.; Schultze, J. D.; Springer, J. *J. Membr. Sci.* **1994**, *90*, 151−159.
(20) Perez, J. *Physique et mécanique des polymères amorphes*; Londres: Paris, 1992.
(21) Angles, M. N.; Dufresne, A. *Macromolecules* **2000**, *33*, 8344−8353.
(22) Gopalan Nair, K.; Dufresne, A. *Biomacromolecules* **2003**, *4*, 657−665.
(23) Stern, S. A. *J. Membr. Sci.* **1994**, *94*, 1−65.
(24) Gontard, N.; Thibault, R.; Cuq, B.; Guilbert, S. *J. Agric. Food Chem.* **1996**, *44*, 1064−1069.
(25) Katz, J. *Z. Phys. Chem.* **1930**, *A150*, 90.
(26) Imberty, A.; Buléon, A.; Tran, V.; Perez, S. *Starch/Stärke* **1991**, *43*, 375−384.

MA050054Z